Applied Surface Science 257 (2011) 6843–6849

Contents lists available at ScienceDirect

Applied Surface Science

journal homepage: www.elsevier.com/locate/apsusc

Hydrogen-free spray pyrolysis chemical vapor deposition method for the carbon nanotube growth: Parametric studies

Mihnea Ioan Ionescu[a], Yong Zhang[a], Ruying Li[a], Xueliang Sun[a,*], Hakima Abou-Rachid[b], Louis-Simon Lussier[b]

[a] Department of Mechanical and Materials Engineering, University of Western Ontario, London, ON. N6A 5B9, Canada
[b] Defense Research & Development Canada – Valcartier, 2459 Boulevard Pie-XI Nord, Québec, QC. G3J 1X5, Canada

ARTICLE INFO

Article history:
Received 30 December 2010
Accepted 1 March 2011
Available online 9 March 2011

Keywords:
Carbon nanotubes
Chemical vapor deposition
Spray pyrolysis

ABSTRACT

Spray pyrolysis chemical vapor deposition (CVD) in the absence of hydrogen at low carrier gas flow rates has been used for the growth of carbon nanotubes (CNTs). A parametric study of the carbon nanotube growth has been conducted by optimizing various parameters such as temperature, injection speed, precursor volume, and catalyst concentration. Experimental observations and characterizations reveal that the growth rate, size and quality of the carbon nanotubes are significantly dependent on the reaction parameters. Scanning electron microscopy, transmission electron microscopy, and Raman spectroscopy techniques were employed to characterize the morphology, structure and crystallinity of the carbon nanotubes. The synthesis process can be applied to both semiconducting silicon wafer and conducting substrates such as carbon microfibers and stainless steel plates. This approach promises great potential in building various nanodevices with different electron conducting requirements. In addition, the absence of hydrogen as a carrier gas and the relatively low synthesis temperature (typically 750 °C) qualify the spray pyrolysis CVD method as a safe and easy way to scale up the CNT growth, which is applicable in industrial production.

1. Introduction

Carbon nanotubes (CNTs) have been extensively studied due to their outstanding electrical, mechanical and optical properties [1–4] which has led to numerous applications of carbon nanotubes as device components, such as sensors [5,6], fuel cells [7–10], field emission devices [11], transistors, and logic circuits [12–14]. Up to now, different techniques including arc discharge, laser ablation and chemical vapor deposition (CVD) have been employed for the CNT growth [15–19]. CVD methods are particularly attractive due to the large area deposition capability, aligned CNT growth, and low costs [20–22]. Among various CVD techniques, spray pyrolysis CVD reveals promising results in CNT synthesis. It provides a controlled way of spraying complex carbonaceous liquids mixed with catalyst containing molecules (metallocene powders) directly into the deposition chamber [23] and ensures semi-continuous growth of CNTs, which gives the possibility to scale up the method for production of CNTs at commercially viable prices. Up to date, high carrier gas flow rates (more than 8000 sccm) have been used in spray pyrolysis experiments and it is still a challenge to obtain catalyst free CNTs with uniform diameters [24,25]. When low carrier gas flow rates were used, the reactant solution could not be sprayed and fully evaporated, leaving behind metallocene residues [26]. To achieve controlled growth of high quality CNTs with uniform size and high yield, a parametric study on the CNT growth in a spray pyrolysis process is necessary. In addition, controlled growth of CNTs on suitable substrates is one of the key impediments in building various nanodevices. Besides CNT growth on conventional silicon substrates, direct growth of CNTs on conducting substrates has been exploited to improve properties of electrode materials. This approach has provided *in situ* electrical end-connection for the individual CNTs and consequently, promises potential applications in fuel-cells, lithium-ion batteries, supercapacitors, sensors, and field emission devices [27]. However, the CNT synthesis on metallic substrates is difficult to achieve mainly due to the degradation of catalytic nanoparticles under the reactive CNT growth conditions, i.e. the hydrogen environment at elevated temperatures. Previously investigated procedures to synthesize CNTs on stainless steel (SS) require intermediated steps associated with substrate preparation prior to CNT growth [28–30].In this work, vertically aligned MWCNTs were achieved on semiconducting Si, conducting carbon microfiber, and stainless steel substrates using a modified spray pyrolysis CVD method without hydrogen addition. Low flow rates of argon carrier gas (175 sccm) were used for micro

* Corresponding author. Fax: +1 519 661 3020.
E-mail address: xsun@eng.uwo.ca (X. Sun).

0169-4332/$ – see front matter © 2011 Elsevier B.V. All rights reserved.
doi:10.1016/j.apsusc.2011.03.011

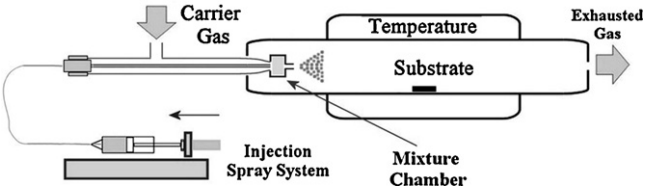

Fig. 1. The spray pyrolysis CVD system.

spraying mixtures of ferrocene in xylene at different concentrations, over substrates situated at growing temperature. Parametric studies on the CNT growth indicated that the nanotube growth was significantly affected by the involved factors such as temperature, injection speed, precursor volume, and concentration of catalyst in carbonaceous precursors. The method offered several significant advantages for instance controlling carrier gas flows without affecting the spraying process, the possibility to use complex mixtures of volatile precursors, the absence of complex substrate preparation, and the setup simplicity. Morphology, structure and crystallinity of nanotubes were investigated using scanning electron microscopy (SEM), transmission electron microscopy (TEM) and Raman techniques. The absence of H_2 as a carrier gas and a relatively low synthesis temperature qualify the spray pyrolysis CVD method as a safe and easy way to scale up route for industrial production.

2. Experimental

The experimental setup was composed of an electronically controlled furnace with 300 mm effective heating length, a quartz reactor tube (i.d. 25.4 mm), and a spraying setup, respectively. The device developed for spraying liquids injected at low flow rates consisted of a carrier gas tube (i.d. 4.2 mm) which ended with a spraying nozzle (i.d. 0.5 mm) and a sealed inner tube (i.d. 1.5 mm) that carried the active solution. The pressure formed inside the carrier gas tube pulverized the solution evenly at low flow rates, through the nozzle, inside the deposition chamber, up to the substrate surface situated in the middle of the quartz tube. The deposition system and the injection device are presented in Fig. 1.

In this parametric study, oriented n-type Si(1 0 0) silicon wafers were used as a substrate, without removing the native oxide layer. An aluminum (Al) under-layer, with the thickness of 30 nm, was magnetron sputtered on the Si substrate to effectively prevent the catalyst particles from aggregation. Effects of growth conditions have been systematically examined by changing one of the following parameters while keeping the others fixed. The investigated parameters were as follows: the growth temperature, injection speed, concentration of ferrocene in xylene, and volume of active solution injected. In the spraying process, argon was used as carrier gas at a flow rate of 175 sccm. After the growth, the reactor was allowed to cool down under argon flow before exposure to air. The same procedure was used for CNT deposition on conducting substrates. Samples were characterized by scanning electron microscopy (SEM – Hitachi S-4800), Raman spectroscopy (Renishaw Raman spectrometer with laser excitation of 785 nm), and transmission electron microscopy (Philips CM-10). The TEM samples were prepared by sonicating a small amount of as-grown nanotubes in ethanol for 10 min and drying few drops of suspension on a Cu micro-grid.

3. Results and discussion

In order to optimize the growth process on Si wafers and conducting substrates, a parametric study was carried out involving perturbation of substrate temperature, injection speed, concentration of catalyst in carbon precursor, and volume injected, while keeping other parameters fixed as described in the experimental part.

3.1. Effect of temperature

CNTs were grown at deposition temperatures in the range of 600–900 °C. All other parameters were kept constant: volume of injected solution at 3 ml, flow rate of carrier argon at 175 sccm, ferrocene/xylene concentration at 1%, and injection speed at 0.75 ml/min.

Fig. 2 shows SEM images of the products obtained at these temperatures. The CNTs could not be produced at 600 °C and only catalyst particles were found on the substrate (Fig. 2a). This suggests that there was insufficient hydrocarbon decomposition below 600 °C and the catalyst particle activity was very low, hindering the CNT formation [31]. The experiments done at 900 °C revealed a substrate covered by amorphous carbon (Fig. 2b), indicating that the iron particles lost their catalytic activity at high temperature. On the other hand, vertically aligned CNT arrays were obtained for all experiments done between these temperatures. The average tube length was 12 μm for 700 °C, increased to 51 μm for 750 °C, and presented a maximum of 63 μm for 800 °C (Fig. 2c). The average diameter of CNTs (Fig. 2d) presented a maximum of 54 nm for tubes synthesized at 700 °C (Fig. 2f) and sharply decreased to 28 nm for tubes grown at 750 °C down to 19 nm for the ones grown at 800 °C (Fig. 2g). At 800 °C, the CNTs were disordered, non-uniform in size, and the diameter distribution was wider due to the agglomeration of the catalyst particles. The Raman spectra for the nanotubes synthesized at 750 °C and 800 °C confirm the degree of crystallinity of the products. The intensity of the G-peak relative to D-peak (I_D/I_G = 0.68, Fig. 2e curve (1)) indicates a higher structural order of tubes synthesized at 750 °C. In comparison, the tubes grown at 800 °C had a weaker line around 1580 cm^{-1} (I_D/I_G = 0.93, Fig. 2e curve (2)) which is a signature of defects contained in graphene walls and a low degree of crystallinity [32].

These results punctuate the temperature influence on the structure of the CNTs. At temperatures lower than 700 °C, the tube growth is inhibited by the low concentration of carbon atoms. Increase of the temperature promotes the decomposition of carbonaceous liquid and CNTs are formed by dissolving, diffusing, and precipitating the carbon atoms trough the catalyst iron particles. The dissolving and diffusion rates increase with temperature and consequently the CNT yield becomes larger. At 900 °C and above, the carbon concentration is too high and the dissolving rate becomes higher than diffusing and precipitating rates. The catalyst particles lose their catalytic activity and the carbon atoms accumulate on the particle surface as amorphous carbon which terminates the CNT growth.

This part of the study demonstrates that VA-CNTs can be synthesized at temperatures in the range of 700–800 °C. While a maximum tube length was obtained at 800 °C, the temperature of 750 °C was the optimum one to grow quality and well-aligned CNT arrays and was considered for the following experiments.

3.2. Effect of injection speed

The effect of injection speed on the CNT growth has been examined in the range of 0.05–1.0 ml/min while keeping other parameters constant. The volume of solution injected was 3 ml, the carrier argon flow rate was 175 sccm, the temperature was 750 °C, and the ferrocene/xylene concentration was 1%. The SEM images show that vertically aligned CNT arrays were obtained for all experiments (Fig. 3a). By increasing the injection speed the tubes became shorter. The average tube length presented a maximum of 237 μm for experiments performed at 0.05 ml/min and decreased to 48 μm for experiments done at injection speed of 1 ml/min (Fig. 3b).

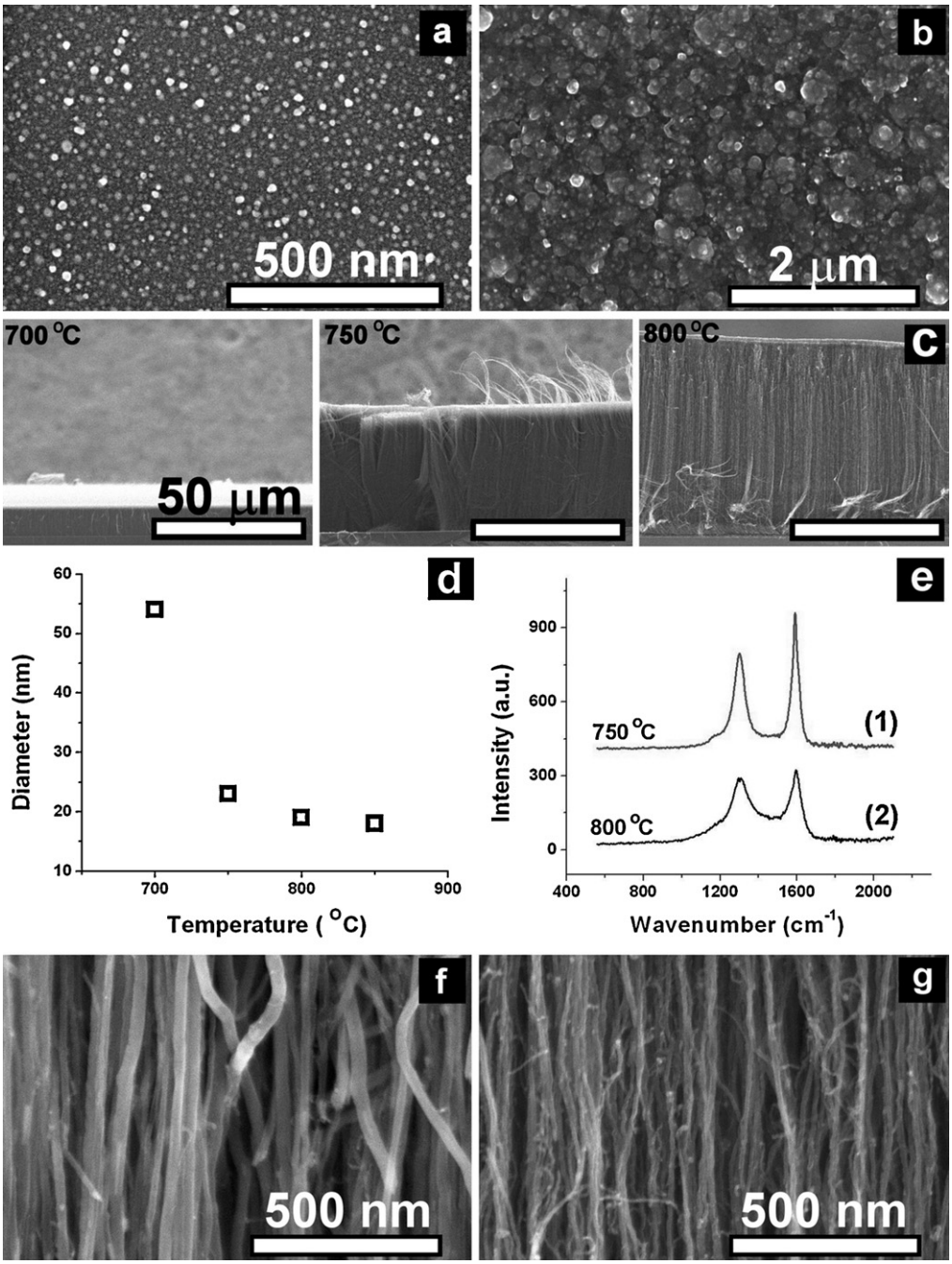

Fig. 2. Substrate temperature influence – CNTs obtained at 600 °C (a); 900 °C (b); VA-CNT array thickness obtained at 700 °C, 750 °C, and 800 °C (c); CNTs average diameter (d); Raman spectra for the nanotubes synthesized at 750 °C and 800 °C (e); CNTs with 54 nm average diameter obtained at 700 °C (f); CNTs with 19 nm average diameter obtained at 800 °C (g).

A higher injection speed shortened the reaction time of the carbonaceous species with the catalyst particles and moderated the catalyst activity. This effect was also reflected on the change of CNT diameters. At low injection speeds, the collisions of the active catalyst nanoparticles were promoted and the iron particles coalesced and formed CNTs with thicker diameters. This effect was weakened for a high injection speed. The average tube diameter was 52 nm for experiments done at the injection speed of 0.05 ml/min and decreased to 18 nm for experiments done at that of 1 ml/min (Fig. 3c). By increasing the injection speed, the length and the average diameter of the CNTs decreased. These are in agreement with previously reported results [33] and indicate that the injection speed has a direct influence over the average length and diameter of CNTs. For the following experiments, the injection speed of 0.1 ml/min was preferred by taking in consideration the length and diameter of obtained CNTs and the easiness to control the injection speed.

3.3. Effect of catalyst concentration

Ferrocene in xylene concentrations in the range of 0.1% and 5% were used to study the influence of the catalyst concentration on the CNT growth. All other parameters were kept constant: volume of solution injected at 3 ml, carrier argon flow rate at 175 sccm, temperature at 750 °C, and the injection speed at 0.1 ml/min. From the SEM images, it can be seen that vertically aligned CNTs arrays were obtained for all experiments (Fig. 4a). The average tube length for

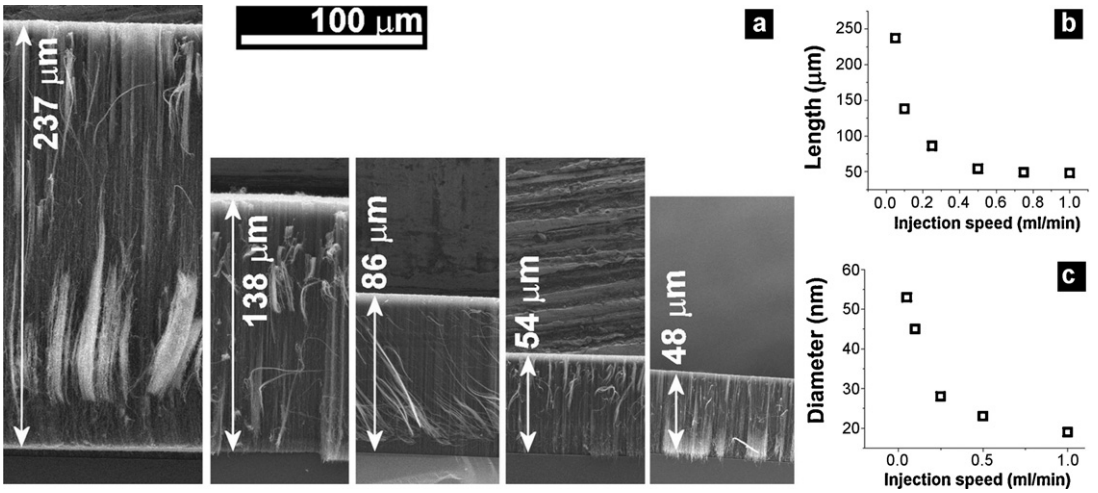

Fig. 3. VA-CNT array thickness obtained at 0.05, 0.1, 0.25, 0.5, and 1.0 ml/min – scale 100 μm (a); average nanotube length function of injection speed (b); average nanotube diameter function of injection speed (c).

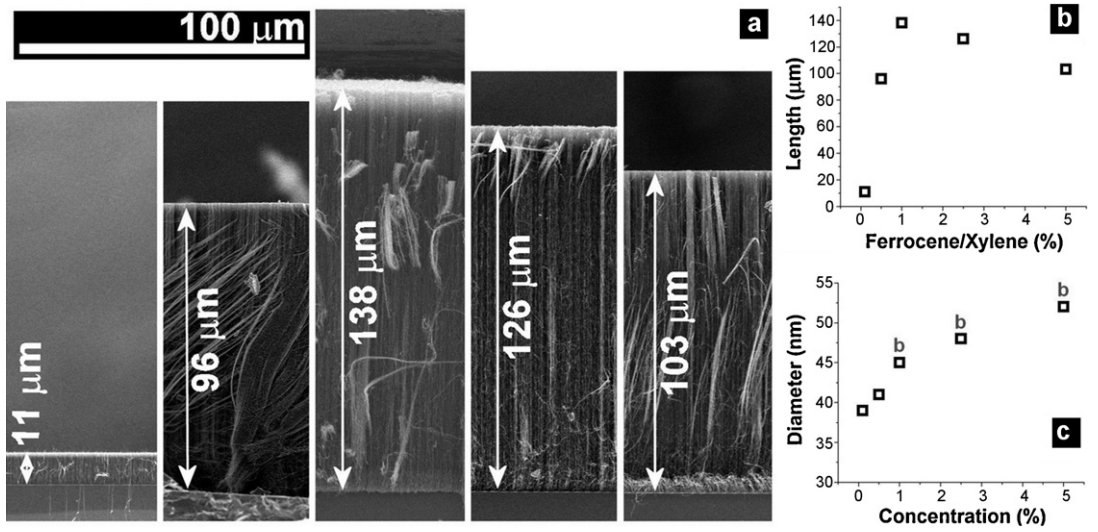

Fig. 4. VA-CNT array thickness obtained using 0.1% ferrocene in xylene, 0.5%, 1%, 2.5%, and 5% (a); average nanotube length (b); average nanotube diameter and the occurrence of bimodal diameter distribution (c).

experiments performed at 0.1% ferrocene in xylene was 11 μm. By increasing the Fe catalyst concentration, the average tube length increased to a maximum of 138 μm for experiments performed at 1% ferrocene in xylene. A future increase of ferrocene concentration decreased the average tube length to 103 μm for experiments done at 5% ferrocene in xylene. These results suggest that an optimum density of iron catalyst nanoparticles and carbon clusters for the nanotube nucleation and growth are obtained when spraying solution with the concentration of 1% ferrocene in xylene (Fig. 4b). In the growth process, some of the sprayed catalyst particles could not reach the substrate and were deposited on the external walls of the formed tubes. Nucleation sites for smaller diameter CNTs are generated and reflected in a bimodal diameter distribution of the samples [34]. The bimodal diameter distribution was observed for all samples synthesized using ferrocene concentrations above 1%. At lower ferrocene concentrations, the bimodal diameter distribution disappeared (Fig. 4c).

SEM and TEM micrographs in Fig. 5 show differences in structure between nanotubes synthesized at 5% and 0.5% ferrocene in xylene concentrations. For high concentrations, the CNTs are non-uniform in size, and the diameter distribution is wider. Besides large nanotubes with the average diameter of 58 nm, the presence of thin nanotubes with the average outer diameter of approximately 24 nm indicates the bimodal diameter distribution of the products (Fig. 5a and b). The larger diameter tubes are spatially aligned while the smaller diameter tubes are entangled. At low ferrocene in xylene concentrations, the CNTs are uniform, with an average diameter of 42 nm diameters, and the bimodal diameter distribution is absent (Fig. 5c and d). The diameter distribution diagram (Fig. 5e) indicates a slight increase of tube diameter and confirms the occurrence of bimodal diameter distribution at high ferrocene concentrations. The Raman spectra for the nanotubes synthesized at 5% and 0.5% concentrations support the TEM observations. The intensity of the D band relative to G band is slightly lower for the nanotubes synthesized at the 0.5% ferrocene in xylene concentration ($I_D/I_G = 0.49$, Fig. 5f curve (1)) in comparison with the nanotubes synthesized at the 5% ferrocene in xylene ($I_D/I_G = 0.67$, Fig. 5f curve (2)) and indicates that the tubes obtained at lower catalyst concentrations present fewer defects and have a higher degree of crystallinity.

3.4. Effect of volume injected

In previous studies, the influence of several reaction parameters on the CNT length was examined by injecting a constant volume of

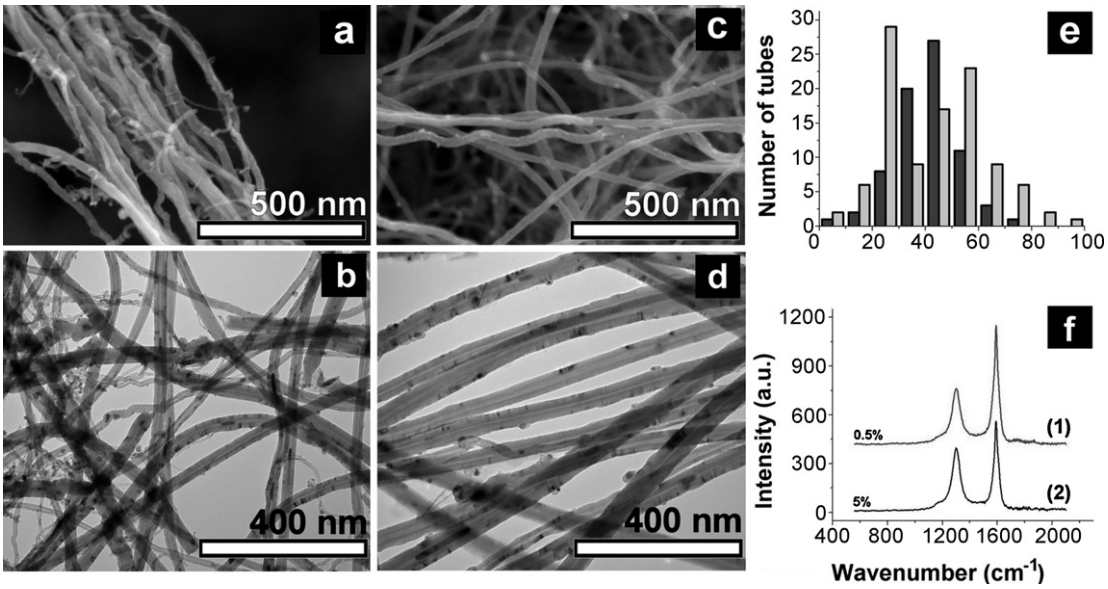

Fig. 5. SEM image for nanotubes synthesized at 5% (a); TEM image for nanotubes synthesized at 5% (b); SEM image for nanotubes synthesized at 0.5% (c); TEM image for nanotubes synthesized at 0.5% (d); diameter distribution of nanotubes obtained at 0.5% and 5% concentrations (e); Raman spectra of nanotubes synthesized at 0.5% and 5% concentrations (f).

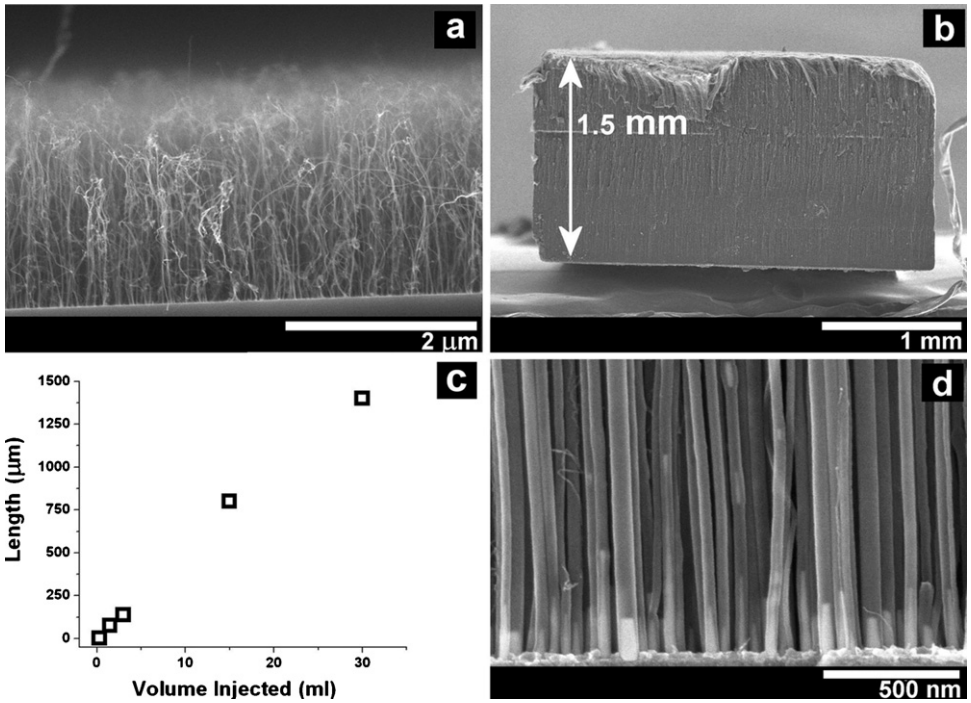

Fig. 6. SEM image for nanotubes synthesized using 0.3 ml active solution (a); SEM image for nanotubes synthesized using 30 ml active solution (b); the average nanotube length (c); SEM image of the nanotube roots (d).

3 ml solution for all experiments. By changing the volume of the injected precursor, using an active solution of 1% concentration, and keeping the other parameters constant as described in the previous experiment, a direct correlation between nanotube length and the volume injected was observed. The nanotube length could be controlled at a range of about three orders of magnitude from 1.7 μm when only 0.3 ml carbon source was injected (Fig. 6a) to 1.5 mm when precursor of 30 ml was injected (Fig. 6b). The variation of the injected volume related with the reaction time indicates almost constant growth rates during the reaction (Fig. 6c). The SEM image of the nanotube array root shows that the catalyst remains on the substrate during the growth process (Fig. 6d). These observations are consistent with all experiments and indicate that the tubes grow upwards following a base growth mechanism.

3.5. *Effect of substrate*

The substrate preparation and growth procedure previously described were applied to conducting substrates, such as carbon paper (CP) and stainless steel 304 (SS). Aluminum was sputtered on CP substrates as previously described. A sheet of SS (Brown Metals Comp.) was cut in 1 cm × 1 cm pieces and used as a substrate with-

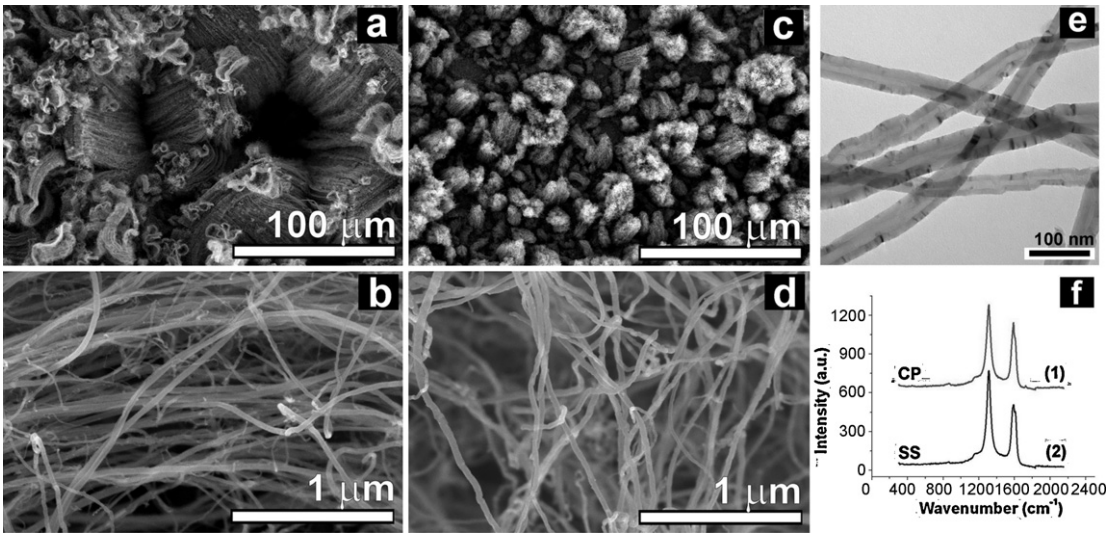

Fig. 7. SEM image of CNTs grown on CP (a and b); SEM image of CNTs grown on SS (c and d); TEM image of CNTs grown on SS (e); Raman spectra of nanotubes synthesized on CP and SS (f).

out additional treatment. The optimized growth conditions used for growing nanotubes on conducting substrates were: ferrocene in xylene concentration of 1%, carrier argon flow rate of 175 sccm, temperature of 750 °C, and injection speed of 0.1 ml/min. Fig. 7 presents SEM images and Raman spectra of the CNTs synthesized by injecting 3 ml volume of solution. A low magnification image of CNTs grown on CP reveals that the substrate was a totally covered with densely aligned tubes with 80–85 μm in length (Fig. 7a) and 5–48 nm in diameter (Fig. 7b), growing along the length of substrate fibers. CNT layer obtained on SS substrate presented dense CNT bundles with the size ranging from one to tens of micrometers (Fig. 7c). The nanotubes were vertically aligned, had lengths up to 30–40 μm, a narrow diameter distribution, and an average diameter of 43 nm (Fig. 7d). Besides the average length, there were no major differences between the obtained products related to TEM images and Raman spectra. The TEM image of the tubes on SS reveals minor structural defects (Fig. 7e) similar to the tubes grown on CP (not shown). This can be assigned to the deficiency of sprayed catalyst to coalesce in uniform particles due to the substrate roughness in comparison with the growth on the Si substrate. The fact that the tubes present more defects is confirmed by Raman investigation which reveals a higher intensity of the D band relative to G band for the tubes grown both on the CP substrate ($I_D/I_G = 1.28$, Fig. 7f curve (1)) and SS substrate ($I_D/I_G = 1.47$, Fig. 7f curve (2)).Previously investigated procedures in terms of synthesizing CNTs on SS conducting substrates have required substrate treatment prior to CNT growth. Typical SS treatment includes acid etching, plasma etching, or treatment in hydrogen atmosphere [28–30]. The spray pyrolysis method reported here does not require additional pretreatment for SS and provides a high CNT yield considering the volume of carbon source used. The catalyst preparation is also bypassed because the catalyst is directly and continuously sprayed over the substrate along with the carbon source. These observations indicate that both CP and SS are efficient conducting substrates for the CNT growth by using spray pyrolysis CVD method.

4. Conclusions

The modified spray pyrolysis chemical vapor deposition has been built in this study. CNTs have been synthesised by the modified spray pyrolysis chemical vapor deposition without hydrogen addition at a low flow rate of carrier gas (175 sccm of argon). The effects of temperature, injection speed, precursor volume, and catalyst/carbon source concentration, have been systematically investigated for optimizing the nanotube growth. The average length and diameter of the carbon nanotubes decreased with temperature and injection speed indicating the possibility of the nanotube growth with controlled structure. The perturbation of catalyst concentration could bring the growth of nanotubes with bimodal diameter distribution and minor effect on tube diameter variation. The optimized growth conditions were applied to semiconducting silicon, conducting carbon paper, and stainless steel substrates. Carbon nanotube forests have been successfully grown on untreated stainless steel substrates. The versatility of this method and the absence of hydrogen usage recommend it as a safe, economical, and easy to scale up route for large-scale production of quality CNTs on different substrates.

Acknowledgements

This research was supported by Department of National Defense (DND), Natural Sciences and Engineering Research Council of Canada (NSERC), Canada Research Chair (CRC) Program, Canada Foundation for Innovation (CFI), Ontario Research Fund (ORF), Ontario Early Researcher Award (ERA), Ontario Graduate Scholarship Program (OGS), and the University of Western Ontario.

References

[1] M.S. Dresselhaus, G. Dresselhaus, P.C. Eklund, Science of Fullerenes and Carbon Nanotubes, Academic Press, San Diego, 1996.
[2] R. Saito, G. Dresselhaus, M.S. Dresselhaus, Physical Properties of Carbon Nanotubes, Imperial College Press, London, 1998.
[3] J. Bernholc, D. Brenner, M.B. Nardelli, V. Meunier, C. Roland, Mechanical and electrical properties of nanotubes, Annu. Rev. Mater. Res. 32 (2002) 347–375.
[4] A. Jorio, G. Dresselhaus, M.S. Dresselhaus, Carbon Nanotubes: Advanced Topics in the Synthesis, Structure, Properties and Applications, Springer, Berlin, 2008.
[5] J. Kong, N.R. Franklin, C. Zhou, M.G. Chapline, S. Peng, K. Cho, H. Dai, Nanotube molecular wires as chemical sensors, Science 287 (2000) 622–625.
[6] S. Ghosh, A.K. Sood, N. Kumar, Carbon nanotube flow sensors, Science 299 (2003) 1042–1044.
[7] X. Sun, R. Li, D. Villers, B.L. Stansfield, J.P. Dodelet, S. Desilets, Composite electrode made of Pt nanoparticles deposited on carbon nanotubes grown on fuel cell backings, Chem. Phys. Lett. 379 (2003) 99–104.
[8] M. Saha, R. Li, X.S Sun, Ye, 3-D composite electrodes of Pt supported nitrogen-doped carbon nanotubes grown on carbon paper for high performance PEM fuel cells, Electrochem. Commun. 11 (2008) 438–441.
[9] M. Saha, R. Li, X. Sun, High loading of Pt nanoparticles on carbon nanotubes as electrodes for PEM fuel cells, J. Power Sources 177 (2008) 314–322.

[10] Y. Chen, J. Wang, H. Liu, R. Li, X. Sun, S. Ye, S. Knights, Enhanced stability of Pt electrocatalysts by nitrogen doping in CNTs for PEM fuel cells, Electrochem. Commun. 11 (2009) 2071–2076.
[11] W. Zhu, C. Bower, O. Zhou, G. Kochanski, S. Jin, Large current density from carbon nanotube field emitters, Appl. Phys. Lett. 75 (1999) 873–875.
[12] T. Rueckes, K. Kim, E. Joselevich, G.Y. Tseng, C.L. Cheung, C.M. Lieber, Carbon nanotube-based nonvolatile random access memory for molecular computing, Science 289 (2000) 94–97.
[13] H.W.C. Postma, T. Teepen, Z. Yao, M. Grifoni, C. Dekker, Carbon nanotube single-electron transistors at room temperature, Science 293 (2001) 76–79.
[14] A. Bachtold, P. Hadley, T. Nakanishi, C. Dekker, Logic circuits with carbon nanotube transistors, Science 294 (2001) 1317–1320.
[15] S. Iijima, T. Ichihashi, Single-shell carbon nanotubes of 1-nm diameter, Nature 363 (1993) 603–605.
[16] C. Journet, W.K. Maser, P. Bernier, A. Loiseau, M. Lamy de la Chapelle, S. Lefrant, P. Deniard, R. Lee, J.E. Fischer, Large-scale production of single-walled carbon nanotubes by the electric-arc technique, Nature 388 (1997) 756–758.
[17] A. Thess, R. Lee, P. Nikolaev, et al., Crystalline ropes of metallic carbon nanotubes, Science 273 (1996) 483–487.
[18] J. Kong, A.M. Cassel, H. Dai, Chemical vapor deposition of methane for single-walled carbon nanotubes, Chem. Phys. Lett. 292 (1998) 567–574.
[19] A.M. Cassell, J.A. Raymakers, J. Kong, H. Dai, Large scale CVD synthesis of single-walled carbon nanotubes, J. Phys. Chem. B 103 (1999) 6484–6492.
[20] K. Hata, D.N. Futaba, K. Mizuno, T. Namai, M. Yumura, S. Iijima, Water-assisted highly efficient synthesis of impurity-free single-walled carbon nanotubes, Science 306 (2004) 1362–1364.
[21] V.K. Kayastha, S. Wu, J. Moscatello, Y.K. Yap, Synthesis of vertically aligned single- and doublewalled carbon nanotubes without etching agents, J. Phys. Chem. C 111 (2007) 10158–10161.
[22] R. Andrews, D. Jacques, A.M. Rao, F. Derbyshire, D. Qian, X. Fan, E.C. Dickey, J. Chen, Continuous production of aligned carbon nanotubes: a step closer to commercial realization, Chem. Phys. Lett. 303 (1999) 467–474.
[23] R. Kamalakaran, M. Terrones, T. Seeger, P.K. Redlich, M. Ruhle, Y.A. Kim, T. Hayashi, M. Endo, Synthesis of thick and crystalline nanotube arrays by spray pyrolysis, Appl. Phys. Lett. 77 (2000) 3385–3388.
[24] C.P. Deck, K. Vecchio, Growth mechanism of vapor phase CVD-grown multi-walled carbon nanotubes, Carbon 43 (2005) 2608–2617.
[25] L.P. Biro, Z.E. Horváth, A.A. Koos, Z. Osvath, Z. Vertesy, Al. Darabont, K. Kertesz, C. Neamtu, Zs. Sarkozi, L. Tapaszto, Direct synthesis of multi-walled and single-walled carbon nanotubes by spray-pyrolysis, J. Optoelectron. Adv. Mater. 5 (2003) 661–666.
[26] C.P. Deck, G.S.B. McKee, K. Vecchio, Synthesis optimization and characterization of multiwalled carbon nanotubes, J. Electron. Mater. 35 (2006) 211–222.
[27] H.S. Kim, B. Kim, B. Lee, H. Chung, C.J. Lee, H.G. Yoon, W. Kim, Synthesis of aligned few-walled carbon nanotubes on conductive substrates, J. Phys. Chem. C 113 (2009) 17983–17988.
[28] D. Park, Y.H. Kim, J.K. Lee, Pretreatment of stainless steel substrate surface for the growth of carbon nanotubes by PECVD, J. Mater. Sci. 38 (2003) 4933–4939.
[29] C. Masarapu, B. Wei, Direct growth of aligned multiwalled carbon nanotubes on treated stainless steel substrates, Langmuir 23 (2007) 9046–9049.
[30] M.D. Abad, J.C. Sanchez-Lopez, A. Berenguer-Murcia, V.B. Golovko, M. Cantoro, A.E.H. Wheatley, A. Fernández, B.F.G. Johnson, J. Robertson, Catalytic growth of carbon nanotubes on stainless steel: characterization and frictional properties, Diamond Relat. Mater. 17 (2008) 1853–1857.
[31] A. Gohier, T.M. Minea, A.M. Djouadi, J. Jimenez, A. Granier, Growth kinetics of low temperature single-wall and few walled carbon nanotubes grown by plasma enhanced chemical vapor deposition, Physica E 37 (2007) 34–39.
[32] M.S. Dresselhaus, G. Dresselhaus, R. Saito, A. Jorio, Raman spectroscopy of carbon nanotubes, Phys. Rep. 409 (2005) 47–99.
[33] L. Tapaszto, K. Kertesz, Z. Vertesy, Z.E. Horvath, A.A. Koos, Z. Osvath, Zs. Sarkozi, Al. Darabont, L.P. Biro, Diameter and morphology dependence on experimental conditions of carbon nanotube arrays grown by spray pyrolysis, Carbon 43 (2005) 970–977.
[34] C. Singh, M.S. Shaffer, A.H. Windle, Production of controlled architectures of aligned carbon nanotubes by an injection chemical vapour deposition method, Carbon 41 (2003) 359–368.